COMPOSITION OF SOME SMECTITES AND DIAGENETIC ILLITIC CLAYS AND IMPLICATIONS FOR THEIR ORIGIN

P. H. NADEAU AND D. C. BAIN

Department of Mineral Soils, The Macaulay Institute for Soil Research
Craigiebuckler, Aberdeen AB9 2QJ, Scotland, United Kingdom

Abstract—Chemical analysis by X-ray fluorescence (XRF) and calculated structural formulae of clay-size fractions of smectites from Cretaceous bentonites and illitic clays from Cretaceous, Devonian, and Ordovician bentonites and Jurassic and Permian sandstones indicate the nature and extent of various types of ionic substitution. The determination of tetrahedral (Al, Si) and octahedral (Al, Mg, Fe) composition shows the variable chemistry of these materials. Structural formulae of the illitic clays show that they have tetrahedral charges between 0.4 and 0.8 per half unit cell, and can be divided into phengitic types having octahedral charges of 0.2–0.4 and muscovitic types having octahedral charges <0.2. Evaluation of the formulae in the light of X-ray powder diffraction (XRD) and transmission electron microscopy (TEM) data shows that the occupancy of non-exchangeable interlayer sites (predominantly K) varies from 47% to 90% of that of ideal muscovite. In some minerals as much as 20% of these sites is occupied by ammonium ions (determined independently). The amount of surface silicate charge balanced by non-exchangeable cations versus that balanced by exchangeable cations has been examined in conjunction with TEM data and suggests that in most samples the charges are about equal. The octahedral composition of smectites in Cretaceous bentonites precludes their having served as transformation precursors for most of the Cretaceous illitic bentonites. The results suggest that these illitic clays originated by neoformation.

Key Words—Bentonite, Chemical composition, Illite, Interstratified, Layer charge, Potassium, Smectite, X-ray fluorescence.

INTRODUCTION

Clay mica, sericite, hydrous mica, and illite are terms that have been used in the literature to refer to clay-size phyllosilicate minerals which are common in soils, sediments, and hydrothermal alteration products. The chemistry and mineralogy of these clays have been widely examined and discussed (Hower and Mowatt, 1966; Weaver and Pollard, 1973; Brown *et al.*, 1978; Środoń and Eberl, 1984). Although these materials have mica-like characteristics, they differ from muscovite in chemical composition (higher Si and Mg, lower Al and K) and in geologic occurrence, which led Grim *et al.* (1937) to propose the name illite as ". . . a general term for clay constituents . . . belonging to the mica group."

Many materials formerly identified as illites have since been shown to contain expandable layers by X-ray powder diffraction (XRD) and are now referred to as interstratified (or mixed-layered) clays, termed illite/smectite (I/S), illite/montmorillonite (I/M), or mica/smectite (M/S). These clays have usually been examined by XRD as oriented, sedimented aggregates that have been solvated with ethylene glycol, thereby expanding the interlayer space of the smectite layers (Figure 1). Calculations based on one-dimensional models of the intensities of the 001 reflections have enabled the layer and type of layer sequence, whether random or regular, to be specified (Reynolds and Hower, 1970; Reynolds, 1980; Środoń, 1980).

The chemistry of illitic clays is no less complicated than their structure. Thus, ionic substitution of Al^{3+}

for Si^{4+} in the tetrahedral sheet and of Mg^{2+} for Al^{3+} in the octahedral sheet may vary significantly, as may the resulting net negative layer charge. Illitic clays are usually dioctahedral and have a half-unit-cell formula of:

$$(K^+E^+)_{x+y}(Al^{3+}_{2-y}Mg^{2+}_y)(Si_{4-x}Al_x)O_{10}(OH)_2,$$
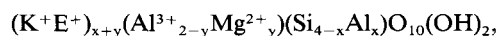
where K^+ refers to non-exchangeable monovalent cations (predominantly K) and E^+ refers to exchangeable monovalent cations (or equivalent divalent cations). Interlayer water (n H_2O) is also present. This formula (modified from Brindley, 1980) is similar to that of dioctahedral smectite and necessarily assumes compositional homogeniety of the 2:1 silicate layers. On this basis, the 4 tetrahedral cations are balanced by 8 oxygens, the 2 octahedral cations by 2 oxygens and 2 hydroxyls, and the non-exchangeable + exchangeable cations, by the net negative layer charge resulting from ionic substitution of Al^{3+} for Si^{4+} (referred to as Al^{IV}) in the tetrahedral sheet (x), and Mg^{2+} for Al^{3+} (referred to as Al^{VI}) in the octahedral sheet (y). An additional complication may be the presence of iron in the octahedral sheet and its oxidation state, which is usually Fe^{3+} in smectites, but which may also be Fe^{2+}, particularly in more illitic clays. The net negative layer charge (x + y) varies from about 0.3 to 0.6 for most smectites and from about 0.5 to 0.9 for most illitic clays.

Interstratified I/S clays in sediments and sedimentary rocks commonly show an increase in their illite content with increasing depth (or inferred depth) of
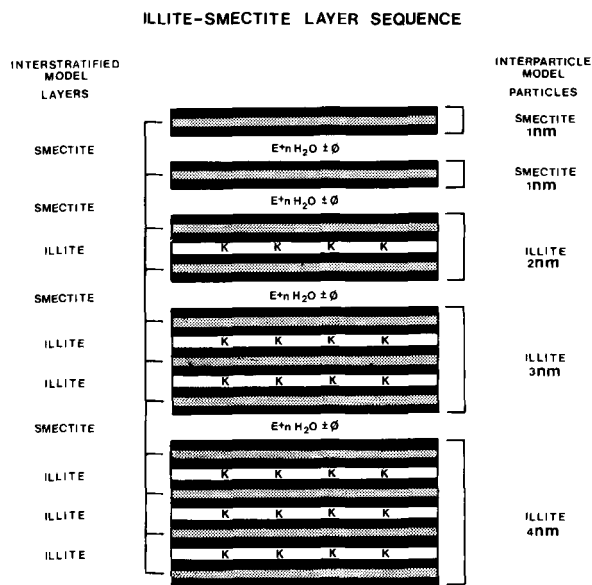
455

ILLITE-SMECTITE LAYER SEQUENCE

Figure 1. Diagrammatic representation of the one-dimensional structure of interstratified illite/smectite layer sequence showing smectite and illite layers as defined by the interstratification model and the equivalent particle sequence as defined by the interparticle model (1 nm = 10 Å). Dark bands represent tetrahedral sheets; stippled bands represent octahedral sheets of the silicate layers; K's are planes of nonexchangeable cations (predominantly potassium), and $E^+nH_2O + \emptyset$ exchangeable cations and interlayer water ± organic molecules such as ethylene glycol or glycerol (not to scale). Note that a single 2:1 silicate layer is identical to an elementary smectite particle in the interparticle model but not identical to a smectite layer in the interstratified model, in which the octahedral sheets are taken as the layer boundaries.

burial (see, e.g., Perry and Hower, 1970; Dunoyer de Segonzac, 1970) and/or proximity to igneous intrusions (see, e.g., Nadeau and Reynolds, 1981). Based on these observations and in combination with chemical and XRD data, a layer-to-layer transformation hypothesis was proposed by Hower *et al.* (1976) in which illite layers form from smectite layers within a fixed layer sequence. This proposed mechanism involves an increase in the net layer charge by a corresponding increase in Al^{IV} (and concomitant decrease in Si^{4+}). The net layer charge may also increase by reduction of octahedral Fe^{3+} to Fe^{2+} (Eslinger *et al.,* 1979). Once the net layer charge is sufficiently large, K^+ is selectively incorporated into the interlayer space, collapsing the smectite layer to form an illite layer. The reaction by this mechanism is:

$$smectite + Al^{3+} + K^+ \rightarrow illite + quartz.$$

A refinement of this model was proposed by Środoń *et al.* (1986).

Recently, a new model was proposed for interstratified clay minerals (Nadeau *et al.,* 1984a, 1984b, 1985a)

which views diagenetic illitic clays as populations of thin phyllosilicate particles. In this model (called the interparticle model), the layer sequence is not fixed within interstratified crystallites. An elementary smectite particle, according to this model, is a single 2:1 silicate layer 1 nm thick (1 nm = 10 Å), and an isolated illite layer is regarded as an elementary illite particle, consisting of two, 2:1 silicate layers coordinated by a single plane of K^+, having a particle thickness of about 2 nm (Figure 1). More extensive illite layer sequences are viewed as thicker illite particles, consisting of n 2:1 silicate layers coordinated by n − 1 planes of K^+, giving a total thickness of about n nm, where n = 3, 4, 5, etc. (Figure 1). Thus, the interparticle model views the layer arrangement as a sequence of particles *within aggregates,* the particle interfaces accounting for the smectite-like adsorption of exchangeable cations, water, and/or organic molecules.

Using the interparticle model, a neoformation hypothesis has been proposed (Nadeau *et al.,* 1984a, 1984b, 1985a) that rationalizes the increases in the proportion of illite layers and the changes in the layer sequences observed in illitic clays during diagenesis. Randomly interstratified I/S layer sequences (<50% illite layers) are thus aggregates consisting of a random sequence of elementary smectite particles and diagenetic elementary illite particles (Nadeau *et al.,* 1984a). As diagenesis proceeds, smectite particles become unstable and dissolve, and the resulting particle population consists primarily of illite particles 2–5 nm thick. Such particle sequences as examined by XRD have been described as regularly interstratified I/S containing >50% illite layers. The mean illite particle thickness increases during later stages of diagenesis, and this increase is perceived by XRD as an increasing number of illite layers. When the mean particle thickness is sufficient (>5 nm) so that XRD no longer detects any expandable layers, the clay is identified as illite *sensu stricto* (as defined by Środoń and Eberl, 1984). The neoformation hypothesis also has implications for the treatment of these materials by chemical activity diagrams (see, e.g., Garrels, 1984). Randomly interstratified I/S is a mixture of two phases, whereas regularly interstratified I/S (>50% illite layers) is a single phase.

The interparticle model and related neoformation hypothesis, therefore, have important chemical implications regarding the mechanism of diagenetic illite formation. The present study attempts to evaluate this model/hypothesis by characterization of the chemical composition of related smectites and illitic clays. Here, 12 Cretaceous smectitic bentonites and 7 Cretaceous illitic bentonites were analyzed by X-ray fluorescence (XRF), and supporting evidence was obtained by XRD and TEM. The smectites are considered to be representative of the clay material in the Cretaceous ben-

Table 1. Sample descriptions.

Sample	Locality	Mineralogy (T_m)[1]
Illitic clays		
SMS	Synthetic NH_4-mica/smectite[2]	70% mica layers (2.93)
C1B, C2B	Cerrillos, New Mexico (MB 211, 737)[3]	70%, 73% illite layers (2.51)
N1B, N2B	New Castle, Colorado (MB 892, 886)[3]	73%, 75% illite layers
ORB	Ophir, Colorado (MB 924)[3]	77% illite layers (2.95)
DIB	Dillon, Colorado (MB 312)[3]	77% illite layers (3.82)
LPB	Las Pedras, Colorado (MB 912)[3]	80% illite layers (3.52)
SFB	St. Francois Mountain, Missouri[4]	80% illite layers (2.57)
RAN	Rannock Formation, North Sea[4]	88% illite layers (3.70)
KAB	Kalkberg Formation, New York[5]	89% illite layers
TGB	Tioga Formation, New York[4]	90% illite layers (4.94)
ROT	Rotliegend Formation, North Sea[4]	100% illite layers (9.22)
Smectites		
WMB	Upton, Wyoming[6]	
LJB	Lake John, Colorado (MB 249)[3]	
R1B, R2B	Rangeley, Colorado (MB 280, 281)[3]	
CRB	Cimarron, Colorado (MB 331)[3]	
HVB	Hanksville, Utah (MB 409)[3]	
MCB	Mt. Carmel, Utah (MB 423)[3]	
GCB	Glen Canyon, Utah (MB 469)[3]	
C3B	Canon City, Colorado (MB 600)[3]	
VLB	Vernal, Utah (MB 819)[3]	
JNB	Jensen, Utah (MB 853)[3]	
RPB	Rio Puerco, New Mexico	

[1] Mineralogy by X-ray powder diffraction of ethylene-glycol-solvated sedimented aggregates using the method of Reynolds (1980). Mean particle thickness (Tm) in nanometers (1 nm = 10 Å) from transmission electron microscopy using the method of Nadeau (1985).

[2] (Wright *et al.*, 1972); [3] Cretaceous bentonites (Nadeau, 1980).

[4] (Nadeau *et al.*, 1985a); [5] Cherry Hill Quarry, from R. C. Reynolds.

[6] (Nadeau *et al.*, 1984c).

tonites prior to their diagenetic conversion to illitic clays. Also analyzed were two filamentous diagenetic illitic clays from sandstones, which were precipitated from pore waters (Wilson and Pittman, 1977; McHardy *et al.*, 1982), three illitic bentonites from Paleozoic carbonate sequences, and a synthetic interstratified clay.

MATERIALS AND METHODS

Relevant details for the 25 samples investigated are listed in Table 1. Bentonite sample designations end with B, samples RAN and ROT are from Jurassic and Permian sandstones, respectively. All of the smectites and 7 of the illitic clays (C1B to LPB, Table 1) are Cretaceous in age, sample TGB is Devonian, and samples SFB and KAB are Ordovician in age.

The clays were Na-saturated using three washes of 1 M NaCl (once overnight) and washed free of Cl^- by centrifugation and/or dialysis. The clay suspensions were size fractionated (<0.1 μm to <2 μm, Tables 2 and 3) and characterized by XRD. The methods of Reynolds (1980) were used to interpret the XRD data of ethylene-glycol-solvated sedimented aggregates (Table 1). The samples were then Ca- and/or Sr-saturated and were analyzed by X-ray fluorescence (XRF) after

ignition at 1000°C. The samples were fused according to the method of Hutton and Elliott (1980) if sufficient material was available (substituting $LiNO_3$ for $NaNO_3$ to enable Na to be determined) or according to the method of Norrish and Hutton (1969). The Kα lines were measured on a Philips PW 1540 spectrometer equipped with a Cr tube (and a Ti filter for the determination of Mn) using pulse-height discriminator settings appropriate to each analytical line. Corrections for background and inter-element effects followed the method of Norrish and Hutton (1969).

Infrared spectroscopy was used to detect structural ammonium ions and to determine semiquantitatively the amounts of silica (quartz, cristobalite/tridymite) and kaolinite present (J. D. Russell, Macaulay Institute for Soil Research, Aberdeen, Scotland, United Kingdom, personal communication). Mössbauer spectroscopy was also used to determine the presence of goethite and hematite as well as ferric and ferrous iron in the silicate minerals. Structural ammonium was determined as nitrogen using pyrolysis-gas chromatography. A further correction had to be made for samples shown to contain structural ammonium, which is lost on ignition at 1000°C.

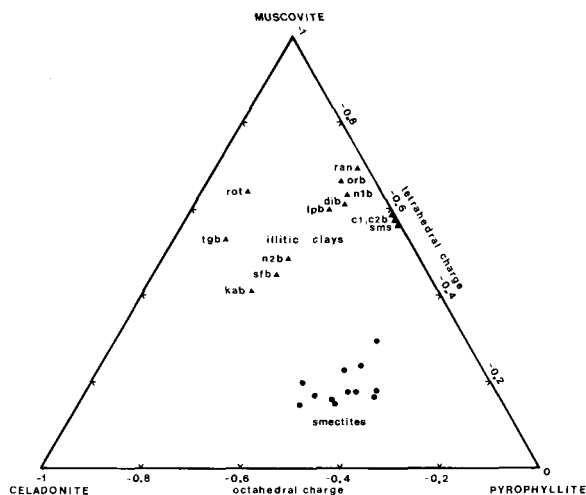Quantitative TEM methods (Nadeau, 1985) were

Figure 2.   Nature of negative charge for illitic and smectite clays illustrated on the muscovite-pyrophyllite-celadonite compositional diagram. Note differences in octahedral charge of the Cretaceous smectites (0.2–0.4) and low octahedral charge (<0.2) of most Cretaceous illitic clays.

used to characterize the <0.1-μm fraction of most of the illitic clays (<0.2-μm fraction for samples DIB, RAN, TGB, and ROT). The mean particle thickness (Tm, Table 1) was determined from 30–55 observations per sample. These finer fractions were also characterized by XRD, if the size fraction for chemical analysis was coarser than that examined by TEM, to ensure that they were virtually the same mineralogically.

RESULTS AND INTERPRETATION

The chemical analyses of the illitic and smectitic samples are shown in Tables 2 and 3, respectively. Structural formulae were calculated (e.g., Gast, 1977) on a half-cell basis consisting of 22 negative charges (i.e., $O_{10}(OH)_2$), after the analyses were corrected for minor amounts of impurities (Tables 2 and 3) where appropriate. It should be noted that the arguments presented here would still be applicable even if these corrections had not been made.

Perhaps the greatest "error" occurred when the analysis was used to calculate a structural formula assuming a single dioctahedral phase, particularly for material identified by XRD as randomly interstratified I/S. According to the interparticle model, this material consists of elementary smectite and illite particles whose chemistry may differ. Such samples were not analyzed. Furthermore, smectites may vary in the degree of ionic substitution in different size fractions (see, e.g., Nadeau et al., 1985b) or may contain small amounts of non-exchangeable K (Table 3) which might indicate the presence of trace amounts of illitic clay not detected by XRD.

Ionic substitution

The chemistry of illites is commonly represented on a muscovite-pyrophyllite-celadonite composition diagram as determined by the structural formulae. These data for the illitic clays show negative tetrahedral charges between 0.4 and 0.8 (Figure 2). Ordovician and Devonian bentonites TGB, KAB, and SFB, Cretaceous bentonites N2B, and Permian sandstone clay ROT plot in a region similar to the published values of illitic clays (see, e.g., Hower and Mowatt, 1966). These clays have octahedral charges between 0.2 and 0.4 and are thus phengitic in character. The remainder of the Cretaceous bentonites and Jurassic sandstone clay RAN have low octahedral negative charges (<0.12); some samples even have slightly positive octahedral charges (Table 2). For plotting purposes in Figure 2, this value was deducted from the tetrahedral charges of clays with positive octahedral charges so that the total net negative charge value shown is correct. Such chemical compositions of illitic clays are not unusual, inasmuch as the chemical data for several Cretaceous illitic bentonites from Montana (Eslinger et al., 1979) show similar characteristics. Such clays are muscovitic in character in that they derive most of their total layer charge from Al^{IV}. The Cretaceous smectites plot in a region of moderate to high overall charge, having octahedral charges of 0.2 to 0.4 and tetrahedral charges of 0.1 to 0.13. The octahedral cation compositions of the Cretaceous smectites and illitic clays differ significantly in their Al^{VI} and Mg^{VI} contents (Figure 3).

Non-exchangeable cation content

A central question about the chemistry of illites is their low K content. Muscovites commonly contain about 10 wt. % K_2O, yet illitic clays usually contain only 4–9% K_2O. The interstratification model accounts for this difference in part by variation in the proportion of illite layers. For example, a clay containing 80% illite layers would contain no more than 80% of the K_2O content of muscovite. Even after this correction, illite layers still have less K than ideal muscovite. This relationship may be evaluated by determining a site occupancy value (So) for the samples in Table 2 by calculating the ratio of non-exchangeable cations (per half cell) to the number of sites available from the proportion of illite layers as determined by XRD. The interparticle model, alternatively, determines the number of available sites by using the mean particle thickness from TEM data (Tm in nm, Table 1) and calculating the ratio of planes of K^+ ions to silicate layers by the expression (Tm − 1)/Tm. Appreciating the necessarily crude nature of this evaluation and that the TEM data for samples ROT, RAN, and TGB are from finer fractions (<0.2 μm) than those on which the chemical analyses were made, the results are shown in Figure 4. An important feature of the data is that TEM consis-

Table 2.   Chemical analyses (wt. %) and structural formulae (half cell) of Ca- or Sr-saturated illitic clays.

	Sample												
	SMS	C1B	C2B	N1B	N2B	ORB	DIB	LPB	SFB	RAN	KAB	TGB	ROT
Size fraction (μm)	<0.2	<2	<0.5	<0.5	<0.5	<0.5	<0.2	<0.1	<0.1	<2	<1	<0.5	<2
SiO_2	53.95	55.26	54.61	53.23	56.76	50.43	54.65	54.29	56.25	52.54	57.30	55.82	53.88
TiO_2	0.01	0.30	0.20	0.36	0.08	0.09	0.12	0.08	0.26	2.02	0.25	0.29	0.12
Al_2O_3	39.55	34.23	33.67	31.87	29.84	32.52	33.14	31.73	27.82	32.13	26.94	29.95	30.18
Fe_2O_3	0.04	2.38	1.49	4.17	1.02	6.74	1.73	1.77	1.35	2.10	0.52	1.11	2.87
FeO	ND	ND	<0.01	ND	0.69	0.17	ND	ND	ND	0.44	0.57	0.19	0.81
MnO	0.03	0.04	0.02	0.07	<0.01	<0.01	0.03	0.04	0.03	<0.01	<0.01	<0.01	<0.01
MgO	<0.01	1.20	1.69	1.81	2.46	1.32	1.32	1.97	3.42	1.98	4.04	2.52	1.64
CaO	<0.01	1.91	0.09	0.01	1.26	<0.01	<0.01	0.08	0.01	0.93	0.94	1.12	0.67
Na_2O	ND	ND	ND	ND	0.14	ND	ND	ND	ND	ND	ND	ND	ND
K_2O	<0.01	4.27	4.67	5.92	6.42	5.20	6.25	5.78	6.39	6.84	7.26	7.05	8.79
$(NH_4)_2O$	2.52	ND	ND	ND	0.26	0.44	0.20	0.31	0.13	ND	0.24	0.84	0.22
P_2O_5	<0.01	0.06	0.05	0.17	0.06	0.02	0.10	0.02	0.09	0.02	<0.01	0.05	0.20
SO_3	<0.01	0.11	0.03	0.06	0.02	<0.01	0.01	<0.01	<0.01	—	<0.01	<0.01	<0.01
SrO	2.96	ND	3.08	2.90	ND	2.40	2.38	2.85	2.46	R	ND	ND	ND
Total	99.05	99.76	100.82	100.57	99.01	99.33	99.92	98.92	98.20	—	98.26	98.94	99.38
LOI	17.43	13.13	12.74	14.32	12.52	11.23	12.41	12.85	14.53	—	10.53	12.84	6.07
Si	3.25	3.37	3.36	3.36	3.52	3.35	3.39	3.41	3.55	3.31	3.59	3.47	3.36
Al	0.75	0.63	0.65	0.64	0.49	0.67	0.61	0.60	0.45	0.70	0.41	0.53	0.64
Tetrahedral charge	-0.75	-0.63	-0.65	-0.64	-0.49	-0.67	-0.61	-0.60	-0.45	-0.70	-0.41	-0.53	-0.64
Al	2.06	1.83	1.79	1.74	1.67	1.89	1.81	1.75	1.62	1.75	1.58	1.67	1.71
Fe^{3+}	—	0.11	0.13	0.12	0.05	0.01	0.08	0.09	0.07	0.10	0.03	0.05	0.07
Fe^{2+}	—	—	—	0.01	0.04	0.01	—	—	—	0.03	0.03	0.01	0.05
Mg	—	0.11	0.16	0.18	0.23	0.13	0.12	0.19	0.32	0.19	0.38	0.24	0.16
Octahedral charge	+0.18	+0.04	+0.06	-0.07	-0.26	-0.07	-0.09	-0.13	-0.31	-0.02	-0.38	-0.37	-0.27
Net layer charge	-0.57	-0.59	-0.59	-0.71	-0.75	-0.69	-0.70	-0.72	-0.76	-0.72	-0.79	-0.90	-0.91
K	—	0.33	0.37	0.49	0.51	0.44	0.50	0.46	0.52	0.57	0.58	0.56	0.74
Na	—	—	—	—	0.03	—	—	—	—	—	—	—	—
NH_4	0.35	—	—	—	0.04	0.07	0.03	0.05	0.02	—	0.07	—	—
Ca	—	0.13	0.01	0.00	0.17	—	0.00	0.01	—	0.07	0.07	0.14	0.04
Sr	0.10	—	0.11	0.11	—	0.09	0.09	0.11	0.09	—	—	0.08	0.05
Interlayer charge	+0.56	+0.58	+0.60	+0.71	+0.73	+0.69	+0.70	+0.73	+0.72	+0.70	+0.78	+0.83	+0.87
CEC	57	68	59	56	45	49	46	55	47	34	33	40	26
Impurities[1]	—	—	1.2g	1.6g 0.5s 1.5k	—	6.6g	—	—	—	2q	—	—	3q 1h

[1] Formula corrected for impurities (wt. %); g = goethite, h = hematite, k = kaolinite, s = silica, q = quartz (see text). ND = not determined; R = recalculated to 100%; LOI = loss on ignition; CEC = meq/100 g.

Table 3. Chemical analyses (wt. %) and structural formulae (half cell) of Ca- or Sr-saturated smectites.

	WMB	LJB	R1B	R2B	CRB	HVB	MCB	GCB	C3B	VLB	JNB	RPB
						Sample						
Size fraction (µm)	<1	<0.5	<0.5	<0.5	<2	<1	<2	<2	<0.5	<2	<2	<0.5
SiO_2	63.12	59.93	62.51	61.16	63.51	61.68	65.48	64.62	62.58	65.34	63.59	63.72
TiO_2	0.13	0.68	0.66	0.39	0.33	0.23	0.13	0.14	0.72	0.26	<0.01	0.12
Al_2O_3	23.06	25.93	22.45	25.03	22.15	23.24	24.00	23.69	23.20	24.07	22.17	25.39
Fe_2O_3	4.01	4.07	3.46	2.95	4.39	2.06	3.66	2.74	2.07	3.23	2.94	2.60
FeO	0.36	ND	ND	ND	ND	ND	ND	ND	0.14	ND	ND	ND
MnO	0.02	0.02	0.01	0.04	0.02	0.01	0.03	0.02	0.03	0.02	0.03	0.02
MgO	2.74	1.94	3.50	3.50	3.45	3.82	3.07	3.76	3.93	3.18	4.11	3.35
CaO	0.01	<0.01	0.01	<0.01	0.10	0.02	3.15	3.55	0.02	3.26	0.01	3.57
Na_2O	0.12	0.09	0.03	ND	0.18	0.09	0.07	0.06	0.14	0.07	0.08	0.11
K_2O	0.01	0.46	0.01	0.24	0.14	0.28	0.01	0.05	0.27	0.04	0.03	0.40
P_2O_5	0.04	0.07	0.08	0.06	0.06	0.06	0.03	0.02	0.03	0.03	0.03	0.03
SO_3	0.02	0.04	0.03	0.03	0.02	0.03	0.01	0.01	0.03	0.01	0.06	0.01
SrO	5.35	5.81	6.44	5.98	6.18	7.36	<0.01	<0.01	7.02	<0.01	6.92	<0.01
Total	98.99	99.04	99.19	99.38	100.53	98.88	99.64	98.66	100.18	99.51	99.97	99.32
LOI	16.77	14.43	14.93	19.85	17.52	16.56	18.51	17.90	17.29	17.47	20.83	18.98
Si	3.82	3.71	3.84	3.77	3.85	3.81	3.84	3.83	3.85	3.83	3.83	3.77
Al	0.18	0.30	0.16	0.24	0.15	0.20	0.17	0.18	0.15	0.18	0.17	0.23
Tetrahedral charge	-0.18	-0.30	-0.16	-0.24	-0.15	-0.20	-0.17	-0.18	-0.15	-0.18	-0.17	-0.23
Al	1.55	1.63	1.50	1.58	1.47	1.54	1.56	1.54	1.51	1.57	1.48	1.59
Fe^{3+}	0.19	0.20	0.17	0.14	0.21	0.10	0.17	0.13	0.10	0.15	0.14	0.12
Fe^{2+}	0.02	–	–	–	–	–	–	–	0.01	–	–	–
Mg	0.26	0.18	0.34	0.32	0.32	0.36	0.28	0.35	0.38	0.29	0.39	0.32
Octahedral charge	-0.24	-0.18	-0.34	-0.22	-0.34	-0.38	-0.25	-0.30	-0.41	-0.28	-0.37	-0.28
Net layer charge	-0.42	-0.48	-0.50	-0.45	-0.49	-0.57	-0.42	-0.48	-0.56	-0.45	-0.54	-0.50
K	0.00	0.04	0.00	0.02	0.01	0.03	0.00	0.01	0.02	0.01	0.00	0.03
Na	0.02	0.01	0.01	–	0.02	0.01	0.01	0.01	0.02	0.01	0.01	0.02
Ca	0.00	0.00	0.00	0.00	0.01	0.00	0.21	0.24	0.00	0.22	0.00	0.23
Sr	0.20	0.21	0.24	0.22	0.22	0.27	0.00	0.00	0.26	0.00	0.26	0.00
Interlayer charge	+0.41	+0.47	+0.49	+0.45	+0.48	+0.58	+0.42	+0.48	+0.56	+0.45	+0.52	+0.50
CEC	106	113	128	115	121	144	115	131	140	119	138	129
Impurities[1]	3s	1s	2s 1k		1.5s	1.5s	2.5s	2s 1k	2.5k 1s	3s	3s	1.5s

[1] Formula corrected for impurities (wt. %); k = kaolinite, s = silica (cristobalite/tridymite, see text). ND = not determined; LOI = loss on ignition; CEC = meq/100 g.
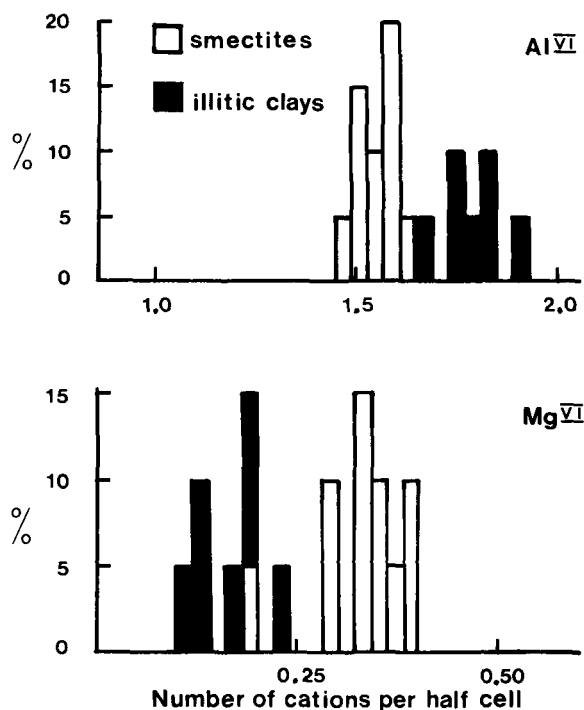
Figure 3. Comparison of octahedral cation compositions of Cretaceous smectite and illitic bentonites. Note differences in Al^{VI} and Mg^{VI} between the two groups.

Figure 4. Relationship between non-exchangeable cation content per half-cell formula unit (K^+) and site-occupancy values using data obtained by X-ray powder diffraction (triangles) and transmission electron microscopy (circles).

tently predicts So values (mean = 0.76) greater than XRD (mean = 0.66). One explanation for this discrepancy is that XRD overestimates the proportion of illite layers. Nevertheless, So values are highly variable and significantly less than unity (i.e., the value for ideal muscovite). Clays with unusually low So values are samples C1B, C2B, and SMS.

For some samples, another factor that might be responsible for low K_2O contents is ionic substitution of NH_4^+ for K^+ in the plane of non-exchangeable cations (Higashi, 1978; Cooper and Abedin, 1981; Cooper and Evans, 1983; Sterne et al., 1982). Analyses by IR of bulk untreated material were also performed to ensure that the NH_4^+ was not an artifact of laboratory contamination (Farmer, 1974). Most clays contain <0.07 NH_4^+ per half cell, but sample TGB contains 0.14 NH_4^+ per half cell. In sample TGB, NH_4^+ comprises 20% of the total non-exchangeable cations. (Partly for this reason, the synthetic NH_4-mica smectite was included in this as a reference.) Even so, nitrogen as non-exchangeable NH_4^+ has been included in the analyses in Figure 4, so this factor alone cannot explain the less-than-ideal So values.

Layer charge

The interstratification model implies that the layer charge is asymmetrically disposed across the 2:1 silicate layer. Smectite layers have a charge of 0.3–0.6 and
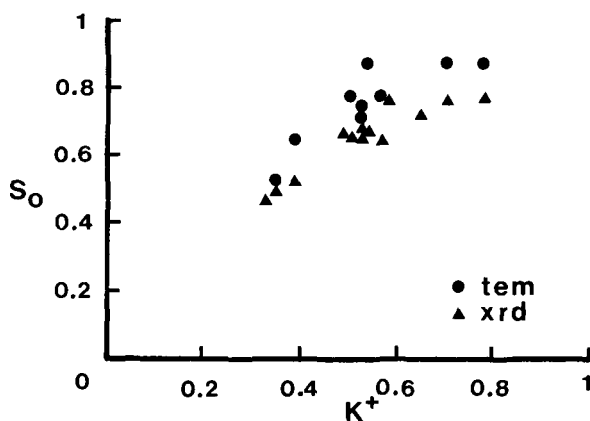
vermiculite layers a charge 0.6–1.0 per half cell, balanced by exchangeable cations. Illite layers have a charge of about 0.5–0.9 and mica layers have a charge of about 1.0, balanced by non-exchangeable cations. Therefore, if a clay is described as a regularly interstratified M/S (mica/smectite), it must be regarded as an alternating sequence of high-charge mica and low-charge smectite layers. Brown (1984) presented such a conceptual model for interstratified clays. As noted above, low So values indicate that an interstratified M/S model is not necessarily applicable on an absolute basis to all illitic clays because So values are significantly less than one. Furthermore, for illitic clays with So <0.6, charge asymmetry does not necessarily exist across the silicate layers in an I/S layer sequence. The asymmetric layer charge model, however, can be evaluated on a relative basis for the illitic clays by comparing the ratio of non-exchangeable to exchangeable cations (K^+/E^+) to the ratio of illite to smectite layers (I:S) as calculated from the XRD data. The assumption is that the charges on the illite and smectite layers are balanced by non-exchangeable and exchangeable cations, respectively.

On the basis of the XRD data (Figure 5a) the asymmetric layer charge predicts that the data should fall consistently below the line of equal charge (equivalence line). Clearly, no such relationship exists. One explanation for this result is that XRD overestimates the proportion of illite layers, as suggested above. For highly illitic clays such an analysis suffers from a similar limitation of the XRD data. A clay identified as containing 100% illite layers by XRD (e.g., sample ROT) still has an exchangeable cation (E^+) content of 0.1/ half cell, corresponding to a cation-exchange capacity (CEC) of 25 meq/100 g. For this sample, the XRD ratio would be infinity, but was taken as 19 for plotting purposes, assuming an XRD accuracy of ±5% (Figure 5a). Other workers have stated that the CEC of such
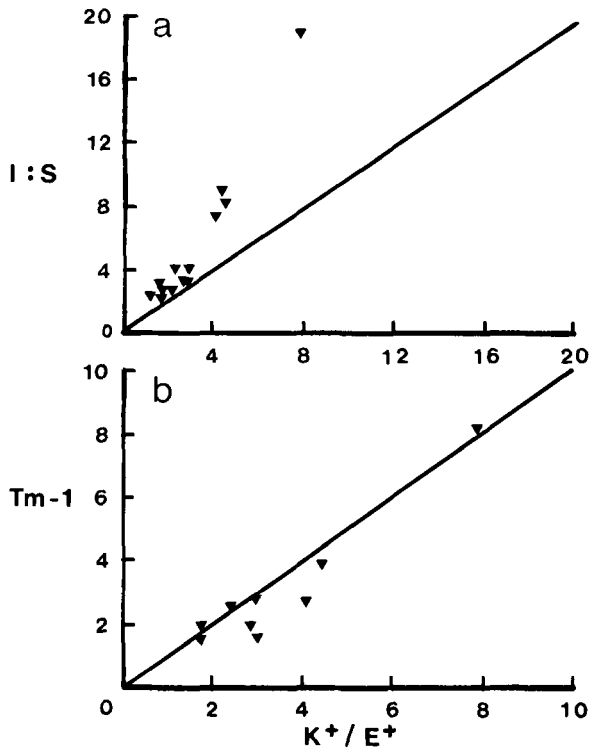
Figure 5. Relationship between ratio of non-exchangeable to exchangeable cations (K^+/E^+, chemical data) and (a) the ratio of illite to smectite layers (I:S, X-ray powder diffraction data), and (b) ratio of planes of non-exchangeable cations and exchangeable silicate interlayers (Tm − 1, transmission electron microscopy data). Equivalents lines (line of equal charge) are shown for comparison.

clays was attributable to non-basal exchange (i.e., edge exchange, Hower and Mowatt, 1966). Quantitative TEM data for sample ROT show that the basal surfaces make up 95% of the total specific surface area of 86 m^2/g (Nadeau, 1985). Thus, the basal surfaces are probably responsible for most of the CEC of this material. The mean particle thickness data (Tm, Table 1), therefore, do not suffer from this limitation and predict the ratio of silicate surfaces with the non-exchangeable cations to those with the exchangeable cations by the expression (Tm − 1). Using these data (Figure 5b), most of the samples plot reasonably close to the equivalence line, suggesting that for these samples the charges across the silicate layers are about equal. Three of the samples, however, fall significantly below the equivalence line, and silicate layer-charge asymmetry may be required to explain the nature of such clays.

DISCUSSION

In general, diagenetic illitic clays in sandstones, such as samples RAN and ROT, are thought to be neoformed materials resulting from the dissolution of K-feldspar and/or kaolinite, whereas illitic clays in

bentonites are thought to have been transformed from smectite, the enclosing sediments providing the external source of K (Altaner *et al.,* 1984). The analyses of the illites from Cretaceous bentonites show that the illitic clays have higher Al^{VI} and lower Mg^{VI} than the "parent" smectites, a feature that is difficult to reconcile with the smectites being transformation precursors of the illitic clays. The transformation hypothesis as defined by Hower *et al.* (1976) predicts that the silicate layer charge increases as a result of Al^{3+}-for-Si^{4+} tetrahedral substitution. In Figure 2, this hypothesis requires that smectites move towards higher layer charge primarily along lines of iso-octahedral charge, or increasing octahedral charge where iron is reduced. Although Cretaceous sample N2B might meet this requirement, the six other Cretaceous illitic clays do not. The data suggest that these clays did not inherit the chemistry of smectite precursors. They are more likely, therefore, to be the products of neoformation. This is not to say that the illitic clays with octahedral charges of 0.2–0.3 are the products of transformation. Sandstone sample ROT has an octahedral charge of 0.27, but such an illitic clay is considered to be neoformed (Wilson and Pittman, 1977). The chemical evidence alone, however, is consistent with both hypotheses. Furthermore, release of Mg and Fe during the diagenetic conversion of smectite to illite, as noted by Boles and Franks (1979), is also consistent with the proposed dissolution of smectite particles.

The chemical data, therefore, suggest that illitic clays in bentonites, like those in sandstones, are neoformed diagenetic products whose chemistry is a consequence of the chemical and physical environment in which they precipitated from solution. This environment is determined by the nature of the sediment, the pore-fluid chemistry, and the thermal and/or burial history. For example, samples from North American Paleozoic carbonate sequences (TGB, KAB, SFB) have octahedral charges of 0.2–0.4, whereas all but one of the Cretaceous bentonites have octahedral charges <0.15 (Figure 2). Similarly, So values of the Paleozoic bentonites are generally higher than those of the Cretaceous bentonites, and the lowest So values are for two bentonites from contact metamorphic environments (C1B, C2B) whose thermal histories are presumably very different from the other bentonites (i.e., they were subjected to higher temperatures for shorter periods of time). Furthermore, the extent of NH_4^+-for-K^+ substitution may be indicative of the amount, type, and degree of thermal alteration of organic matter within the host sedimentary sequences. Thus, the higher Si and Mg and lower K and Al contents of illitic clays relative to ideal muscovite should be related to the chemical and physical diagenetic conditions prevailing at the time of their crystallization. These conditions are almost certainly very different from those of muscovites formed in ig-

neous and high-grade metamorphic rocks. The variable chemistry of illitic clays may reflect the wide variety of diagenetic environments in which they form. Further research is required, however, to understand better such possible relationships.

A consequence of this limited study is that the expandable layers of many illitic clays is due to 2:1 silicate layers whose charges are significantly greater than 0.6, i.e., charges usually found for vermiculite layers. The distinction between smectite-like and vermiculite-like behavior using a layer charge boundary of 0.6 may not necessarily be appropriate for diagenetic illitic clays. Thus, it may be preferable to refer to these layers simply as "expandable," without specifying a particular mineralogy or layer charge.

CONCLUSIONS AND SUGGESTIONS FOR FURTHER WORK

The chemistry of many illitic clays cannot readily be reconciled with an origin via a layer-by-layer transformation from precursor smectite. A diagenetic neoformation mechanism is favored for the origin of these clays whereby they precipitated from aqueous solution. The chemistry of these materials may reflect in part the nature of the chemical and physical diagenetic environment in which they formed as influenced by the host sediments, pore fluids, and thermal and/or burial history. Future research should attempt to establish relationships between such environments and the extent of ionic NH_4^+-for-K^+, Al^{3+}-for-Si^{4+} and Mg^{2+}-for-Al^{3+} substitution, as well as the presence and oxidation state of iron in illitic clays. Furthermore, experimental and theoretical research should attempt to establish the effects of these chemical parameters on the thermodynamic stability as well as the kinetic growth/dissolution rates by which these phyllosilicate minerals achieve, or attempt to achieve, equilibrium.

ACKNOWLEDGMENTS

REFERENCES

Altaner, S. P., Hower, J., Whitney, G., and Aronson, J. L. (1984) Model for K-bentonite formation: evidence from zoned K-bentonites in the disturbed belt, Montana: *Geology* **12**, 412–415.

Boles, J. R. and Franks, S. G. (1979) Clay diagenesis in Wilcox sandstones of southwest Texas: implications of smectite diagenesis on sandstone cementation: *J. Sed. Pet.* **49**, 55–70.

Brindley, G. W. (1980) Order-disorder in clay mineral structures: in *Crystal Structures of Clay Minerals and their X-ray Identification,* G. W. Brindley and G. Brown, eds., Mineralogical Society, London, 125–195.

Brown, G. (1984) Crystal structures of clay minerals and related phyllosilicates: *Phil. Trans. Royal Soc. Lond. A* **311**, 221–240.

Brown, G., Newman, A. D. C., Rayner, J. H., and Weir, A. H. (1978) The structures and chemistry of soil clay minerals: in *The Chemistry of Soil Constituents,* D. J. Greenland and M. H. B. Hayes, eds., Wiley, Chichester, 29–178.

Cooper, J. E. and Abedin, K. Z. (1981) The relationships between fixed ammonium-nitrogen and potassium in clays from a deep well in the Texas Gulf Coast: *Texas J. Sci.* **33**, 103–111.

Cooper, J. E. and Evans, W. S. (1983) Ammonium-nitrogen in Green River Formation oil shale: *Science* **219**, 492–493.

Dunoyer de Segonzac, G. (1970) The transformation of clay minerals during diagenesis and low grade metamorphism: a review: *Sedimentology* **15**, 281–376.

Eslinger, E. V., Highsmith, P., Albers, D., and deMayo, B. (1979) Role of iron reduction in the conversion of smectite to illite in bentonites in the disturbed belt, Montana: *Clays & Clay Minerals* **27**, 327–338.

Farmer, V. C. (1974) The layer silicates: in *The Infrared Spectra of Minerals,* V. C. Farmer, ed., Mineralogical Society, London, 331–363.

Garrels, R. M. (1984) Montmorillonite/illite stability diagrams: *Clays & Clay Minerals* **32**, 161–166.

Gast, R. G. (1977) Surface and colloid chemistry: in *Minerals in Soil Environments,* J. B. Dixon and S. B. Weed, eds., Soil Science Society of America, Madison, Wisconsin, 27–73.

Grim, R. E., Bray, R. H., and Bradley, W. F. (1937) The mica in argillaceous sediments: *Amer. Mineral.* **22**, 813–829.

Higashi, S. (1978) Dioctahedral mica minerals with ammonium ions: *Mineralogical J.* **9**, 16–27.

Hower, J., Eslinger, E. V., Hower, M., and Perry, E. A. (1976) Mechanism of burial metamorphism of argillaceous sediments: I. Mineralogical and chemical evidence: *Geol. Soc. Amer. Bull.* **87**, 725–737.

Hower, J. and Mowatt, T. C. (1966) The mineralogy of illites and mixed-layer illite/montmorillonites: *Amer. Mineral.* **51**, 825–854.

Hutton, J. T. and Elliott, S. M. (1980) An accurate XRF method for the analysis of geochemical exploration samples for major and trace elements using one glass disc: *Chemical Geol.* **29**, 1–11.

McHardy, W. J., Wilson, M. J., and Tait, J. M. (1982) Electron microscope and X-ray diffraction studies of filamentous illitic clays from sandstones of the Magnus field: *Clay Miner.* **17**, 23–39.

Nadeau, P. H. (1980) Burial and contact metamorphism in the Mancos Shale: Ph.D. thesis, Dartmouth College, Hanover, New Hampshire, 200 pp.

Nadeau, P. H. (1985) The physical dimensions of fundamental clay particles: *Clay Miner.* **20**, 499–514.

Nadeau, P. H., Farmer, V. C., McHardy, W. J., and Bain, D. C. (1985b) Compositional variations of the Unterrupsroth beidellite: *Amer. Mineral.* **70**, 1004–1010.

Nadeau, P. H. and Reynolds, R.C. (1981) Burial and contact

metamorphism in the Mancos Shale: *Clays & Clay Minerals* **29,** 249–259.

Nadeau, P. H., Tait, J. M., McHardy, W. J., and Wilson, M. J. (1984c) Interstratified XRD characteristics of physical mixtures of elementary clay particles: *Clay Miner.* **19,** 67–76.

Nadeau, P. H., Wilson, M. J., McHardy, W. J., and Tait, J. M. (1984a) Interstratified clays as fundamental particles: *Science* **225,** 923–925.

Nadeau, P. H., Wilson, M. J., McHardy, W. J., and Tait, J. M. (1984b) Interparticle diffraction: a new concept for interstratified clays: *Clay Miner.* **19,** 757–769.

Nadeau, P. H., Wilson, M. J., McHardy, W. J., and Tait, J. M. (1985a) The conversion of smectite to illite during diagenesis: evidence from some illitic clays from bentonites and sandstones: *Mineral. Mag.* **49,** 393–400.

Norrish, K. and Hutton, J. T. (1969) An accurate X-ray spectrographic method for the analysis of a wide range of geological samples: *Geochim. Cosmochim. Acta* **33,** 431–453.

Perry, E. A. and Hower, J. (1970) Burial diagenesis in Gulf Coast pelitic sediments: *Clays & Clay Minerals* **18,** 165–177.

Reynolds, R. C. (1980) Interstratified clay minerals: in *Crystal Structures of Clay Minerals and their X-ray Identification,* G. W. Brindley and G. Brown, eds., Mineralogical Society, London, 249–303.

Reynolds, R. C. and Hower, J. (1970) The nature of inter-layering in mixed-layer illite-montmorillonites: *Clays & Clay Minerals* **18,** 25–36.

Środoń, J. (1980) Precise identification of illite/smectite interstratifications by X-ray powder diffraction: *Clays & Clay Minerals* **28,** 401–411.

Środoń, J. and Eberl, D. D. (1984) Illite: in *Micas, Reviews in Mineralogy 13,* S. W. Bailey, ed., Mineralogical Society of America, Washington, D.C., 495–544.

Środoń, J., Morgan, D. J., Eslinger, E. V., Eberl, D. D., and Karlinger, M. R. (1986) Chemistry of illite/smectite and end-member illite: *Clays & Clay Minerals* **34** (in press).

Sterne, E. J., Reynolds, R. C., and Zantop, H. (1982) Natural ammonium illites from black shales hosting a stratiform base metal deposit, Delong Mountains, northern Alaska: *Clays & Clay Minerals* **30,** 161–166.

Weaver, C. E. and Pollard, L. D. (1973) *The Chemistry of Clay Minerals:* Elsevier, Amsterdam, 5–23.

Wilson, M. D. and Pittman, E. D. (1977) Authigenic clays in sandstones: recognition and influence on reservoir properties and paleoenvironmental analysis: *J. Sed. Pet.* **47,** 3–31.

Wright, A. C., Granquist, W. T., and Kennedy, J. V. (1972) Catalysis by layer silicates. I. The structure and thermal modification of a synthetic ammonium dioctahedral clay: *J. Catalysis* **25,** 65–80.